

Advanced Microchannel Radial Receivers for the Economic Feasibility of Solar Thermal Power Plants

SolarPACES

María José Montes^{1,*} , José Ignacio Linares² , David D'Souza¹ , Mercedes Ibarra¹ ,
Eva Arenas^{2,3} , Alexis Cantizano^{2,3} , Marta Muñoz¹ , Rubén Barbero¹ ,
and Antonio Rovira¹ 

¹National University of Distance Education (UNED), C/ Juan del Rosal 12, 28040 Madrid, Spain

²Comillas Pontifical University (COMILLAS), Alberto Aguilera 25, 28015 Madrid, Spain

³Institute for Research in Technology, Comillas Pontifical University, Spain

*Correspondence: María José Montes, mjmontes@ind.uned.es

Abstract. A key aspect for the development of solar thermal technology is to improve cost-competitiveness without compromising efficiency. One of the more expensive items in a solar thermal power plant is the heliostat field, which accounts for 40-50% of the total plant investment. One way to decrease this cost is to reduce the size of the field by improving the efficiency in the thermal exploitation of this concentrated solar radiation.

This work presents a novel radial solar receiver design based on compact structures, which allows solar radiation to be absorbed more efficiently by reducing the absorber area and shaping a macroscopic sun trap geometry to reduce heat losses. These compact structures are specially designed to work with pressurised gases, so their coupling to supercritical CO₂ power cycles is straightforward. Specifically, the direct coupling to a novel sCO₂ cycle is considered, where the heat is supplied in the low-pressure line of the cycle and the CO₂ is compressed at low temperature, which reduces the auxiliary consumption, increasing the net efficiency.

The advantages of the microchannel radial receiver have been highlighted by a thermo-economic comparison between this receiver and a conventional external receiver, resulting in a significantly lower total plant investment (171 Mio.\$ vs. 195 Mio.\$). This difference is due to the smaller heliostat field required, due to the improved thermal performance of the novel receiver design compared to the more conventional one.

Keywords: Central Solar Receiver, Microchannel Radial Receiver, Compact Structure, Pressurised Gas, Supercritical Fluid, Supercritical Cycle, Thermo-Economic Analysis

1. Introduction

According to IRENA [1], the Levelised Cost of Energy (LCOE) of Solar Thermal Power Plants (STPPs) was reduced by 68% between 2010 and 2022, mainly due to lower investment and O&M costs. While the LCOE can be reduced by lowering costs, there is another approach to make Concentrated Solar Power (CSP) competitive: increasing the overall efficiency of the STPP. In this way, the CSP Gen3 programme [2] identifies, as one of the most promising

schemes, the coupling between a supercritical CO₂ cycle (S-CO₂ cycle) and a central receiver system. Depending on the Heat Transfer Fluid (HTF) used in the solar receiver, the following research lines can be identified: advanced molten salts, liquid metals, solid particles, gases and supercritical phases. This work has focused on a scheme based on a novel S-CO₂ cycle coupled to a central receiver system, exploring the possibility of a new receiver concept, a microchannel radial receiver, and comparing this design to a conventional external tubular receiver, as depicted in Figure 1.

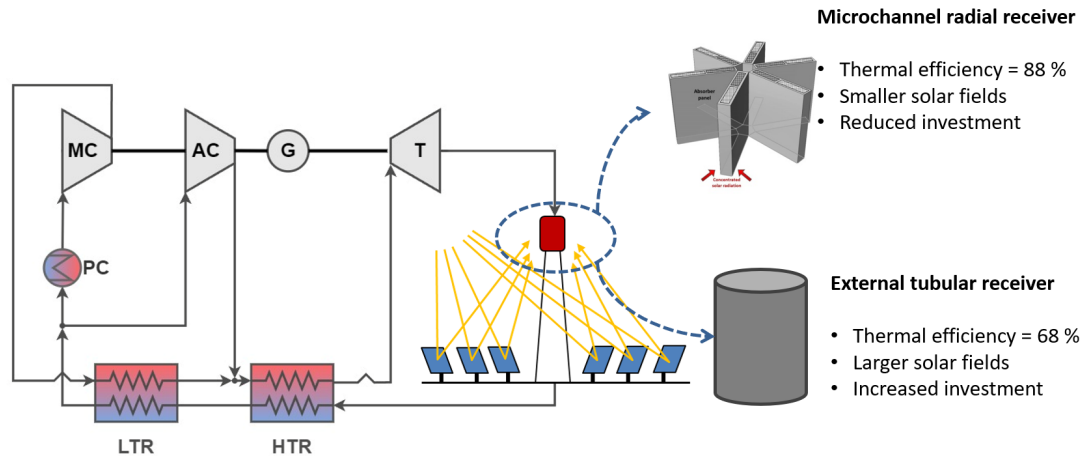


Figure 1. Schematic of the microchannel radial receiver and the conventional external tubular receiver integrated into the S-CO₂ power cycle

Pressurised gas solar receivers have been studied for decades [3]. The most conventional concept is the external tubular receiver, highlighting the tubular cavity designs developed in Solgate, Solhyco and Solugas project [4]. In addition to tubular designs, the compact solar receiver or microchannel receiver is a more recent design that is being widely studied for both pressurised gases and supercritical fluids. It offers the advantage of increasing the heat transfer area between the HTF and the receiver walls. This type of receiver is based on compact structures such as those used in Compact Heat Exchangers (CHE). The state of the art during the last decade of compact solar receivers for pressurised gases and supercritical fluids begins with a review by Li et al. [5] on compact structures applied to solar receivers. From there, several simulation models, reviews and prototypes can be cited, including the 3 MW_{th} receiver presented by Besarati et al. [6] and the 2 MW_e receiver developed by the National Renewable Energy Laboratory (NREL) [7].

In this work, a novel design of a compact solar receiver is proposed, which consists of a radial configuration of absorber panels based on compact structures of increasing compactness [8], as shown in Figure 2. In the proposed design, the bladed receiver concept is applied, so that the absorber panels converge on the tower axis, and the concentrated solar radiation is incident on both sides of each absorber panel. This configuration has already been proposed for tubes; in that case, the panel can experience deformations and bending at high radiation fluxes, due to the thin-walled design of the tube. The novelty of this proposal is based on applying the bladed concept to absorber panels formed by compact structures. This feature overcomes one of the main drawbacks of compact solar receivers, which is the high thermal gradient across the absorber panel thickness due to the low thermal conductivity of the standard materials currently used in these structures. Besides that, all previous designs proposed to date consider uniform compactness [9], that is, the hydraulic diameter is uniform across all channels within the panel; however, as shown in Figure 2, the increasing compactness of the proposed design consists in reducing the hydraulic diameter of the channels from one pass to the next in the fluid heating direction, increasing the turbulence and improving the cooling. Finally, it is important to note that the number of panels is not limited to six. The number of panels is the result of an optimization process, explained in [10,11].

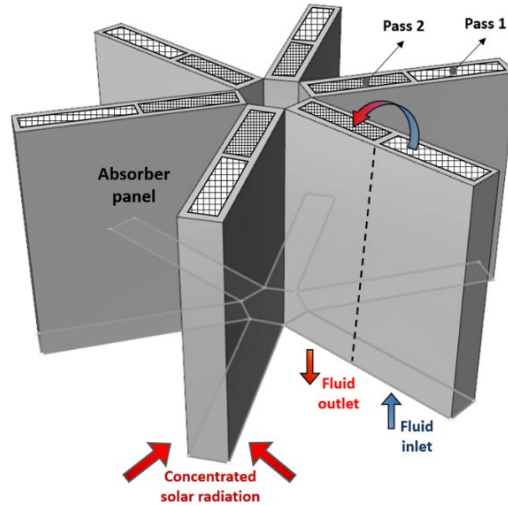


Figure 2. Schematic of the microchannel radial solar receiver based on compact structures

2. Methodology

This work presents an economic comparison at design conditions (Seville, Spain, at solar noon on 21st March; ambient temperature = 25°C, Direct Normal Irradiation (DNI) = 900 W/m²) of two 50 MW_e STPPs based on the same novel S-CO₂ cycle [12], coupled directly to a central receiver system; thus, the operation conditions at the solar receiver (inlet pressure and temperature, and outlet temperature) are the same. The only difference between the two configurations lies in the solar receiver design, as the microchannel radial receiver will be compared to a conventional external tubular receiver.

2.1 A novel S-CO₂ cycle coupled to the central solar receiver system

The selected power cycle is a direct-coupled S-CO₂ recompression cycle with low-pressure solar heat supply, described by Linares et al. [12] and depicted in Figure 3. This cycle is based on the recompression scheme, so two compressors are included: the Main Compressor (MC), which supplies CO₂ at high pressure to the Low Temperature Recuperator (LTR); and the Auxiliary Compressor (AC), which connects to the High Temperature Recuperator (HTR). The main difference between this cycle and a conventional recompression cycle lies in the position in which the solar thermal energy is supplied. In this case, it is supplied downstream of the turbine (T), on the low-pressure side of the cycle, and the CO₂ pressure is therefore much lower than in a conventional recompression cycle. In addition, the cycle includes air cooling by means of a corresponding Pre-Cooler (PC).

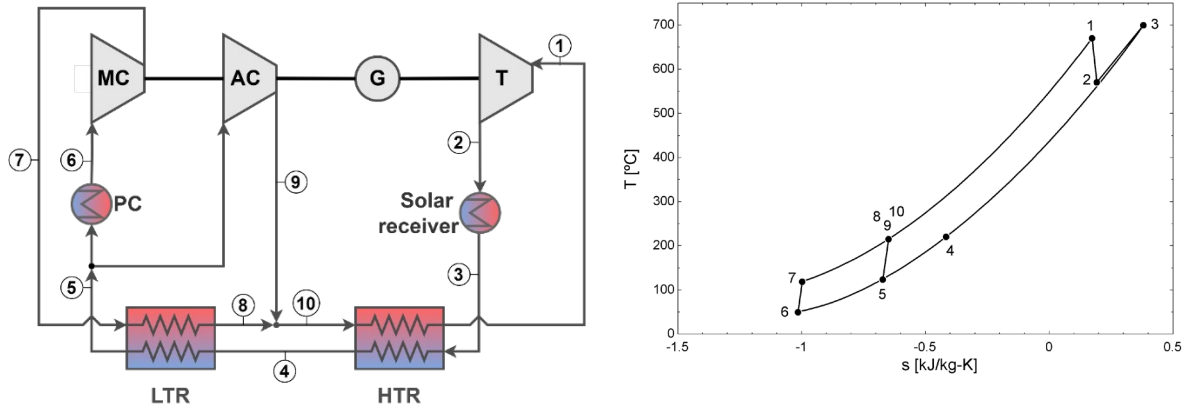


Figure 3. Schematic of the S-CO₂ cycle with direct coupling and low-pressure solar heat supply (Source: [12]).

Table 1 summarises the thermodynamic properties of the points marked on the S-CO₂ cycle diagram shown in Figure 3.

Table 1. Properties and state points of the novel S-CO₂ cycle

State points	P (bar)	T (°C)	h (kJ/kg)
1	276.4	665	669.2
2	96.42	525.3	506.6
3	90.31	700	721.1
4	88.5	335	284.1
5	86.73	152.9	75.31
6	85	50	-80.9
7	287.8	147.4	-20.01
8	282	329.5	244.5
9	282	284.8	186.3
10	282	320	232.3
Net power (MW_e)	50		
Thermal power (MW_{th})	117.64		
Net cycle efficiency (%)	42.5		

As shown in the table, the net electrical power is 50 MW_e. The net cycle efficiency is the ratio between the net power of the cycle and the thermal power input. The net power is calculated as the gross power minus the internal consumptions of the cycle: compressors and the PC fan, as shown in Eq. (1).

$$\eta_{net,cycle} = \frac{\dot{W}_{net,cycle}}{\dot{Q}_{th,receiver}} = \frac{\dot{W}_{gross,cycle} - \dot{W}_C - \dot{W}_{fan}}{\dot{Q}_{th,receiver}} \quad (1)$$

2.2 Thermal and geometric parameters of the solar receivers

As previously said, the design conditions are the same for both receivers. The required thermal power is 117.64 MW_{th} and the CO₂ inlet conditions to the receiver are equal to 96.42 bar and 525.3 °C, with the outlet target temperature of 700 °C, as calculated in the previous section. The tower height is also the same for both STPPs, since it is calculated on the basis of the thermal power [9]. The material for the tubes in the external receiver or the compact structure

in the microchannel receiver is Nickel-based alloy Inconel 740H [13]. Both receivers are considered to be covered by Pyromark (solar absorptivity of 0.96 and thermal emissivity equal to 0.88).

The maximum velocity through the tubes or through the channels of the second fluid pass of the compact structure is set to the maximum allowed to avoid vibration problems [14], according to the following Eq. (2). The first fluid pass of the compact structure is designed considering a maximum velocity equal to half the velocity of the second pass.

$$u_{max} = \frac{175}{(\rho_f(750^\circ\text{C}))^{0.43}} \quad (2)$$

The expression for energy efficiency is the same for both receivers, Eq. (3), and is defined as the useful heat transferred to the working fluid divided by the solar heat incident on the receiver.

$$\eta_{en,receiver} = \frac{\dot{Q}_{th,HTF,receiver}}{\dot{Q}_{solar,receiver}} \quad (3)$$

The other geometric or thermo-fluid dynamic parameters are specific to each of the receiver designs and are described below.

2.2.1 External tubular receiver

The external tubular receiver has been designed according to the design guidelines for this type of receiver, taking into account that the working fluid is supercritical CO₂ [13, 15]. The external diameter (d_o) is set to 1 inch, and the minimum tube wall thickness is calculated according to ASME Boiler and Pressure Vessel Code [16]. The aspect ratio (receiver height-to-diameter, for external receivers) is set to 1.5 and the view factor is equal to 1, as the outer surface directly irradiates to ambient. Table 2 shows the main geometric parameters, as well as the results of the thermo-fluid dynamic simulation.

Table 2. Geometric and thermo-fluid dynamic parameters of the external tubular receiver

Geometric parameters	
Receiver height (m)	17.69
Receiver diameter (m)	11.8
Number of tubes	1459
Outer tube diameter (mm)	25.4
Tube wall thickness (mm)	4.18
Thermofluid-dynamic parameters	
Maximum fluid velocity (m/s)	32.16
Average incident solar flux (MW/m ²)	0.16
Pressure drop (bar)	3.39
Heat loss (MW _{th})	53.12
Radiation heat loss (MW _{th})	44.69
Reflection heat loss (MW _{th})	1.65
Convection heat loss (MW _{th})	6.78
Energy efficiency (%)	68.65
Exergy efficiency (%)	44.76

2.2.2 Microchannel radial receiver

The microchannel receiver design has been optimised according to the guidelines described in [10]. The thermal model of the microchannel receiver is explained in depth in [10,11]. The optimal number of panels is calculated to be 6; one of the panels is south-facing, and the other converging panels are distributed in such a way that the angle between them is equal. The aspect ratio (receiver height-to-twice the cavity radius, for cavity receivers) is set to 0.7. The geometry of the considered compact structure is plain rectangular fin type, so the channels are squared, with the channel side size of the second fluid pass being half the channel side size of the first fluid pass. This design increases the fluid velocity and improves the cooling of the panel close to the tower axis, which is the one exposed to a higher concentrated solar flux. Table 3 shows the main geometric and thermal parameters.

Table 3. Geometric and thermofluid-dynamic parameters of the microchannel radial receiver

Geometric parameters	
Number of panels.	6
Panel height (m)	6.1
Panel width (m)	4.36
Pass 1 channel dimensions (mm x mm)	12 x 12
Pass 2 channel dimensions (mm x mm)	5 x 5
View factor for absorber panel area (pass 1)	0.68
View factor for absorber panel area (pass 2)	0.39
Thermofluid-dynamic parameters	
Pass 1 maximum fluid velocity (m/s)	16.08
Pass 2 maximum fluid velocity (m/s)	32.15
Average incident solar flux (MW/m ²)	0.42
Pressure drop (bar)	6.49
Total heat loss (MW _{th})	15.28
Radiation heat loss (MW _{th})	10.98
Reflection heat loss (MW _{th})	2.53
Convection heat loss (MW _{th})	1.77
Energy efficiency (%)	88.55
Exergy efficiency (%)	56.04

Comparing Table 2 and Table 3, it can be observed that the energy efficiency of the radial receiver is higher than that of the conventional external receiver, mainly due to a reduction in radiation heat losses. This reduction is due to the cavity effect created between two converging panels, which is also favoured because the area of the panel with a higher surface temperature is the one close to the tower axis, which has a lower view factor to the outside.

2.3 Calculation of the solar field coupled to each solar receiver

Once the dimensions of the solar receivers are calculated, an optical simulation of the heliostat field is conducted using the SolarPILOT and Soltrace programs [17]. The aim point strategy for both receivers is the same, and it is the one adopted by SolarPILOT to calculate the heliostat field for a single external receiver. Then, this heliostat field is exported to Soltrace. In the case of the conventional external receiver, the solar flux map is directly calculated by Soltrace, while in the case of the microchannel receiver, the hypothetical external receiver is replaced by the corresponding convergent absorber panels, to properly calculate the solar flux map on these panels. Table 4 shows the main solar field data for both receivers. As can be seen in

this table, the optical efficiency is higher in the case of an external tubular receiver compared to a microchannel receiver (mainly due to its larger absorber surface); however, the number of heliostats is also much higher, since a greater incident solar heat on the receiver is required, as its energy efficiency is lower.

Table 4. Optical parameters of the solar field coupled to each receiver

	Microchannel receiver	External tubular receiver
Tower height (m)	112.62	112.62
Receiver absorber area (m²)	159.46	247.45
Number of heliostats	1642	2043
Optical efficiency (%)	82.4	85.41

3. Results and conclusions

Table 5 shows the main economic results of the STPPs based on each of the solar receiver designs. The solar field data has been calculated through SolarPILOT, while the cycle cost has been calculated in a previous work [18], and is equal in both cases, amounting to 90.27 Mio.\$.

Table 5. Economic results for the STPP based on microchannel receiver vs external receiver

Costs (Mio.\$)	Microchannel receiver	External tubular receiver
Tower	10.71	10.71
Receiver	20.77	28.25
Site improvements	3.79	4.72
Heliostat field	34.37	42.77
Contingency	4.92	7.98
Total direct cost	74.57	94.43
Land	3.73	5.8
Sales tax	3.16	5.11
Total indirect cost	6.89	10.91
Total solar system	81.46	105.34
Total power cycle	90.27	90.27
Total STPP	171.73	195.61

As shown in Table 5, the microchannel radial receiver results in a lower total investment in the STPP (171 Mio.\$ vs. 195 Mio.\$), mainly because a smaller heliostat field is required, as this receiver is more compact and has a higher efficiency than a conventional external receiver.

It should be noted that the average incident solar flux values considered in this work are lower than those typically reported for commercial molten-salt receivers. This is a deliberate design choice, as the study focuses on pressurised CO₂ receivers, whose heat transfer and thermo-mechanical constraints require more conservative flux levels. Therefore, the conclusions of this work are valid within the context of gas/supercritical-fluid receivers, and should not be extrapolated to molten-salt-based technologies.

Author contributions

M. J. Montes: conceptualization; data curation; formal analysis; funding acquisition; investigation; methodology; project administration; resources; software; supervision; validation; visualization; writing – original draft; writing – review & editing. J. I. Linares: conceptualization; data curation; formal analysis; funding acquisition; investigation; methodology; project administration; resources; software; supervision; validation; visualization; writing – original draft; writing – review & editing. D. D’Souza: investigation; methodology; software; writing – review & editing. M. Ibarra: investigation; methodology; software; writing – review & editing. E. Arenas: investigation; methodology; software; writing – review & editing; funding acquisition; project administration. A. Cantizano: investigation; methodology; software; writing – review & editing. M. Muñoz: investigation; methodology; software; writing – review & editing. R. Barbero: investigation; methodology; software; writing – review & editing. A. Rovira: investigation; methodology; software; writing – review & editing; funding acquisition; project administration.

Competing interests

The authors declare that they have no known competing financial interests or personal relationships that could have appeared to influence the work reported in this paper.

Data availability statement

The data that support the findings of this study are available from the corresponding author upon reasonable request.

Underlying and related material

No underlying or supplementary material is associated with this article.

Funding

Project supported by the Spanish Ministry of Science and Innovation through the PID2019-110283RB-C33 and PID2019-110283RB-C31 projects.

Project also supported by the BBVA Foundation's Leonardo Scholarship for Researchers and Cultural Creators 2024. The BBVA Foundation is not responsible for the contents, comments and opinions included in the project and/or the results derived from it, which are the full and absolute responsibility of their authors

References

- [1] IRENA (2023), "Renewable power generation costs in 2022", International Renewable Energy Agency, Abu Dhabi.
- [2] M. Mehos *et al.*, "Concentrating Solar Power Gen3 Demonstration Roadmap", NREL/TP-5500-67464, 1338899, ene. 2017. <https://doi.org/10.2172/1338899>
- [3] C.K. Ho, 2017. "Advances in central receivers for concentrating solar applications". *Sol. Energy* 152, 38–56. <https://doi.org/10.1016/j.solener.2017.03.048>
- [4] R. Korzynietz, et al., 2016. Solugas – Comprehensive analysis of the solar hybrid Brayton plant. *Solar Energy* 135, 578–589. <https://doi.org/10.1016/j.solener.2016.06.020>
- [5] Q. Li, G. Flamant, X. Yuan, P. Neveu, L. Luo, 2011. "Compact heat exchangers: A review and future applications for a new generation of high temperature solar receivers". *Renew. Sustain. Energy Rev.* 15, 4855–4875. <https://doi.org/10.1016/j.rser.2011.07.066>

- [6] S.M. Besarati, D. Yogi Goswami, E.K. Stefanakos, 2015. "Development of a Solar Receiver Based on Compact Heat Exchanger Technology for Supercritical Carbon Dioxide Power Cycles". *J. Sol. Energy Eng.* 137, 031018. <https://doi.org/10.1115/1.4029861>
- [7] S.D. Sullivan, J. Kesseli, J. Nash, J. Farias, D. Kesseli, W. Caruso, 2016. "High-Efficiency Low-Cost Solar Receiver for Use in a Supercritical CO₂ Recompression Cycle" (No. DOE-BRAYTON--0005799, 1333813). <https://doi.org/10.2172/1333813>
- [8] M.J. Montes, A. Rovira, J. González-Aguilar and M. Romero, 2022. "Solar receiver consisting of absorber panels based on compact structures". Spanish Patent ES2911108. PCT application n. PCT/ES2022/070705. Eu. application n. 2023/10572
- [9] J.E. Hesselgreaves, 2017. *Compact heat exchangers: selection, design, and operation*, Second edition. ed. Elsevier/BH, Amsterdam.
- [10] M.J. Montes, R. Guédez, D. D'Souza, J.I. Linares, J. González-Aguilar, M. Romero, 2023. "Proposal of a new design of central solar receiver for pressurised gases and supercritical fluids". *Int. J. Therm. Sci.* 194, 108586. <https://doi.org/10.1016/j.ijthermalsci.2023.108586>
- [11] M.J. Montes, R. Guédez, D. D'Souza, J.I. Linares, 2023. *Thermoeconomic Analysis of Concentrated Solar Power Plants Based on Supercritical Power Cycles*. *Applied Sciences* 13, 7836. <https://doi.org/10.3390/app13137836>
- [12] J.I. Linares, M.J. Montes, A. Cantizano, C. Sánchez, 2020. "A novel supercritical CO₂ recompression Brayton power cycle for power tower concentrating solar plants". *Appl. Energy* 263, 114644. <https://doi.org/10.1016/j.apenergy.2020.114644>
- [13] M. Fernández-Torrijos, P.A. González-Gómez, C. Sobrino, D. Santana, 2021. "Economic and thermo-mechanical design of tubular sCO₂ central-receivers". *Renew. Energy* 177, 1087–1101. <https://doi.org/10.1016/j.renene.2021.06.047>
- [14] NORSOK standards <https://www.standard.no/petroleum> (2024)
- [15] M. Laporte-Azcué, P.A. González-Gómez, M.R. Rodríguez-Sánchez, D. Santana, 2021. "Material selection for solar central receiver tubes". *Sol. Energy Mater. Sol. Cells* 231, 111317. <https://doi.org/10.1016/j.solmat.2021.111317>
- [16] American Society of Mechanical Engineers, *Boiler and Pressure Vessel Code*, 2024
- [17] M.J. Wagner, T. Wendelin, 2018. "SolarPILOT: A power tower solar field layout and characterization tool". *Sol. Energy* 171, 185–196. <https://doi.org/10.1016/j.soler.2018.06.063>
- [18] J.I. Linares, E. Arenas, M.J. Montes, A. Cantizano, J.R. Pérez-Domínguez, J. Porras, 2024. "Direct coupling of pressurized gas receiver to a brayton supercritical CO₂ power cycle in solar thermal power plants". *Case Stud. Therm. Eng.* 61, 105021. <https://doi.org/10.1016/j.csite.2024.105021>